Journal of Nuclear Materials 398 (2010) 146–152

Contents lists available at ScienceDirect

Journal of Nuclear Materials

journal homepage: www.elsevier.com/locate/jnucmat

Corrosion investigations of Al–Fe-coated steels, high Cr steels, refractory metals and ceramics in lead alloys at 700 °C

Abu Khalid Rivai [a,*], Minoru Takahashi [b,1]

[a] Department of Nuclear Engineering, Graduate School of Science and Engineering, Tokyo Institute of Technology, N1-18, 2-12-1, O-okayama, Meguro-ku, Tokyo 152-8550, Japan
[b] Research Laboratory for Nuclear Reactors, Tokyo Institute of Technology, N1-18, 2-12-1, O-okayama, Meguro-ku, Tokyo 152-8550, Japan

A B S T R A C T

Corrosion tests of several types materials were carried out in lead–bismuth eutectic and lead at 700 °C. Al–Fe-coated SUS316FR, and high Cr steels SUS430, Recloy10 and NTK04L were tested in molten lead–bismuth and Al–Fe-coated STBA26, high Cr steel STBA26, refractory metals tungsten and molybdenum and ceramics SiC and Ti_3SiC_2 were tested in molten lead. Oxygen concentrations were 5×10^{-6} and 4.5×10^{-7} wt.% for the molten lead–bismuth and lead, respectively. The unbalanced magnetron sputtering (UBMS) technique was adopted for the coating with targets of Al and SUS304. The results showed that a very thin oxide layer was formed on the coating layer and protected the material from corrosion attack lead alloys. On the other hand, penetration attack of lead alloys into the base of the high Cr steels was observed. The refractory metals and the ceramics exhibit high corrosion resistance to high temperature lead at 700 °C.

1. Introduction

The advantages of liquid lead–bismuth (Pb–Bi) eutectic and lead (Pb) from chemical, physical, thermal hydraulic and neutronics properties have been well known as well as the corrosion problem of these alloys [1–3]. The issue of compatibility of core, proton beam window and structural materials with the lead–bismuth eutectic (LBE) and lead has to be solved in order to realize the development of lead alloy-cooled fast reactors and accelerator driven system. Therefore, the development of high corrosion-resistant materials with LBE and lead environment is one of the key issues for the development of LBE and lead nuclear systems.

Research and development of materials compatible with high temperature LBE and lead have been performed by several researchers [1–21]. The materials selection in these various tests and experiments, surface-coated steels, high Cr steels, refractory metals and ceramics, are all potential candidate materials for LBE and lead nuclear systems.

Several researchers reported the effectiveness of surface-treated steels with various aluminum alloying techniques to protect steels from corrosion in LBE and lead. Aluminum alloying on surfaces by heating-up Al-foil wrapping [4,5], surface-melting with a pulsed electron beam [6,7], the gas diffusion method [8], and pack cementation [9] showed good corrosion resistance in the lead alloys. In the previous investigation [4–9] the temperature of LBE and lead was below 650 °C. At a higher temperature of lead alloy, an Al–Fe-coated steel using UBMS (unbalanced magnetron sputtering technique) method was reported good corrosion resistance in lead–bismuth at 700 °C [10]. Corrosion behavior of high chromium steels in molten LBE and lead has been investigated. The high chromium steels showed good corrosion resistance in the lead alloys [11–17]. At a higher temperature of lead alloy investigation, FeCrAlY steel showed good corrosion resistance after exposed in lead at 700 °C for more than 13,000 h [17]. Corrosion behavior of refractory metals and ceramics in molten LBE and lead has been investigated. Refractory metals of tungsten and molybdenum [10,17,19], and ceramics of SiC [10,11,19] and Ti_3SiC_2 [10,20,21] was reported good corrosion resistance in the lead alloys.

As reviewed above, valuable information has been reported for surface-treated steels, high Cr steels, refractory metals and ceramics for the development of LBE and lead nuclear systems. Corrosion investigation of these materials has been done in the LBE and lead mainly up to 650 °C. However, investigations on corrosion behavior of these materials in LBE and lead at temperature above 650 °C have been few. In the present study, corrosion behavior was investigated for Al–Fe-coated steels using UBM sputtering technique, high Cr steels, refractory metals and ceramics in molten LBE and lead at a temperature of 700 °C.

* Corresponding author. Present address: Nuclear Transmutation Technology Group, J-PARC, Japan Atomic Energy Agency, Tokai-mura, Naka-gun, Ibaraki-ken 319-1195, Japan. Tel.: +81 29 282 6026; fax: +81 29 282 5671.
E-mail addresses: rivai.abukhalid@jaea.go.jp (A.K. Rivai), mtakahas@nr.titech.ac.jp (M. Takahashi).
[1] Tel./fax: +81 3 5734 2957.

0022-3115/$ - see front matter © 2009 Elsevier B.V. All rights reserved.
doi:10.1016/j.jnucmat.2009.10.025

2. Experimental set-up and procedure

2.1. Experimental apparatus and procedure

A pot-type LBE and lead test apparatus was used for the corrosion tests as shown in Fig. 1. The detail of corrosion test apparatus has already been described in Ref. [10]. The apparatus consists of a corrosion test section, a steam generator, a moisture sensor, a heater section and a gas exhaust system for the gas injection, and an oxygen sensor for measurement of oxygen potential in the LBE and lead. The oxygen sensor was made of sintered ceramic zirconia, i.e. magnesia–stabilized zirconia ($MgO–ZrO_2$) and yttria–stabilized zirconia ($Y_2O_3–ZrO_2$). The internal reference in the cell of the oxygen sensor was oxygen-saturated bismuth fluid made from initial powder mixture of 95 wt.%Bi–5 wt.%Bi_2O_3.

Experimental conditions are shown in Table 1. The specimens were immersed in molten LBE and lead at 700 °C. The LBE was 45%Pb and 55%Bi eutectic and purity of the lead was 99.99%. The LBE and lead impurities are shown in Table 2. Oxygen concentrations were controlled to be 5×10^{-6} and 4.5×10^{-7} wt.% for LBE and lead, respectively. These concentrations were determined from the measured EMF and the Gromov's oxygen solubility equation [1].

After immersion of the specimens in the LBE, the specimens were immersed in hot glycerin at 160–180 °C to remove the residual LBE, while those tested in the lead were not. The glycerin was removed from the surfaces of the specimens using water at 70–80 °C. Afterwards, the specimens were cut through the middle and embedded in resin. The cross sections of the specimens were polished with a mechanical grinder using polycrystalline diamond grains of up to 1 μm fine polishing step. Finally, the specimen cross sections were observed by a scanning electron microscope (SEM) and analyzed by an energy-dispersive X-ray (EDX) analysis.

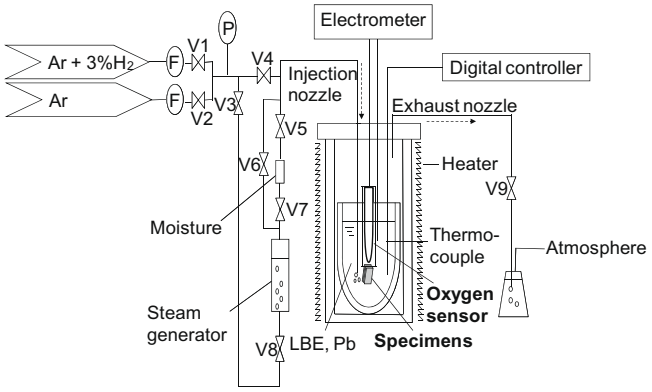

Fig. 1. Schematic of corrosion test apparatus.

Table 1
Experimental conditions.

Parameter	Pb–Bi	Pb
Temperature (°C)	700	700
Oxy. concent. (wt.%)	5×10^{-6}	4.5×10^{-7}
Tested materials		
Coated steel	Al–Fe-sputtering coated SUS316FR	Al–Fe-sputtering coated STBA26
High Cr steel	SUS430, Recloy10, NTK04L	STBA26
Refractory metal	–	Mo, W
Ceramic	–	SiC, Ti_3SiC_2
Immersion time (h)	1000	500

2.2. Test materials

Materials tested were Al–Fe-coated steels, high Cr steels, refractory metals and ceramics. The chemical compositions of the specimens are shown in Table 3 and corrosion test condition of each specimen is shown in Table 1. The shapes of the specimens were rectangular with $15 \times 15 \times 2$, $10.7 \times 9.5 \times 2$, $10 \times 5 \times 2$, $10 \times 5 \times 2.3$, $15 \times 10 \times 1$, $4.6 \times 5.2 \times 1.6$, $6 \times 9.8 \times 2$, $10.2 \times 4.2 \times 2$, $9.6 \times 5 \times 2.3$, and $10.2 \times 4 \times 1.3$ mm in sizes, for Al–Fe-coated SUS316FR, Al–Fe-coated STBA26, SUS430, Recloy10, NTK04L, STBA26, tungsten, molybdenum, SiC and Ti_3SiC_2, respectively. The high chromium steels are in generally corrosion resistance in lead alloys at temperature up to 550 °C according to previous research, and those containing Si and Al are more promising steels than the others. Tungsten, molybdenum and SiC were supplied by the Nilaco Company. The Ti_3SiC_2, one of the new types of solids with 4.5 g/cm^3 in density [22], was supplied by the 3-ONE-2 LLC. Prior to exposure, the surfaces of the high chromium steels, the refractory metals and the ceramics specimens were polished with a mechanical grinder using polycrystalline diamond grains of up to 1 μm fine polishing step.

Al–Fe was coated on the surface of SUS316FR and STBA26 by physical vapor deposition (PVD) using the Unbalanced Magnetron Sputtering (UBMS) method. The UBM sputtering method which was adopted in this study has already been described in Ref. [10]. Two plates of Al and SUS304 were used as the targets and were bombarded by Ar ions with increased concentration in non-equilibrium magnetic fields generated by the magnetic source. Sputtered atoms from the targets deposited on the surfaces of steel specimens. Fig. 2a and b shows the SEM micrograph of the cross section of the Al–Fe-coated SUS316FR and STBA26 as received which were not immersed in lead alloys. The thicknesses of the coating layer are about 20 and 10 μm for Al–Fe-coated SUS316FR and STBA26, respectively. These specimens were coated at the same time and under the same conditions with the specimens that were immersed in the LBE and lead. These figures show that the coating layer is adhered to the surface of SUS316FR and STBA26.

3. Results

3.1. Corrosion test in lead–bismuth eutectic

Fig. 3a–h shows the SEM-EDX micrographs of the cross sections of the tested specimens after immersion in molten lead–bismuth for 1000 h. Fig. 3a shows the SEM micrograph of the cross section of the Al–Fe-coated SUS316FR. The coating layer can be identified by its darker color. It was found that the coating layer (darker color) of about 20 μm in thickness still remained on the surface of the

Table 2
Impurities of LBE and lead (unit: wt.%).

	Cu	Ag	Au	Sn	Zn	Fe	As	Sb	Bi
LBE	1.4×10^{-3}	8.8×10^{-4}	2.2×10^{-4}	2.2×10^{-4}	6.9×10^{-4}	1.8×10^{-3}	–	–	–
Lead	$<10^{-4}$	$<10^{-4}$	–	$<10^{-4}$	$<10^{-4}$	$<10^{-4}$	$<10^{-4}$	$<10^{-4}$	$<10^{-4}$

Table 3
Chemical compositions of the specimens (unit: wt.%).

		Cr	Mo	Ni	Mn	Si	Al	C	P	S
High chromium steels	SUS430	16.13	–	–	0.20	0.63	–	–	–	–
	Recloy10	17.69	–	–	0.68	0.99	0.89	0.01	0.24	0.003
	NTK04L	17.84	–	–	0.14	0.41	3.34	0.002	0.022	0.001
	STBA26	9	1	–	–	0.2	–	–	–	–
	SUS316FR	18	2	12	–	–	–	<0.02	–	–
Coated steels	Targets: Al–SUS304 (18 Cr, 8 Ni, bal. Fe)									
Refractory metals	W	99.95 purity								
	Mo	99.95 purity								
Ceramic	SiC	98 SiC–0.2 SiO_2–0.1 Si–1.2 C								

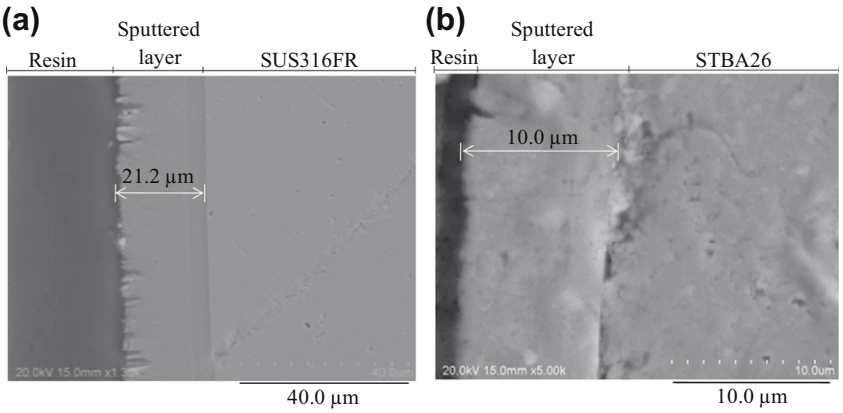

Fig. 2. (a) SEM micrograph of cross section of Al–Fe-coated SUS316FR as received. (b) SEM micrograph of cross section of Al–Fe-coated STBA26 as received.

SUS316FR specimen with no penetration of LBE. Fig. 3b shows the result of the EDX micrograph analysis for atomics distribution. The O, Al, Cr, and Fe atoms were enriched on the surface layer. The peak of oxygen atoms on the surface suggested that a very thin oxide layer was formed on the surface of the coating layer. The formation of the oxide layer on the surface of Al–Fe coating layer because the present coating layer was formed by using Al and SUS304 steels sputtering targets. The SUS304 mainly contains iron and about 18 wt.% chromium. The oxygen concentration in LBE of this experiment was 5×10^{-6} wt.% which was higher than the formation potentials of aluminum oxide, chromium oxide and iron oxide at 700 °C. Therefore, alumina oxide, chromium oxide, and iron oxide were possibly formed during immersion in LBE. This very thin and stable oxide layer acted as a barrier against corrosion attack by LBE. The oxide layer protects the surface of the coating layer from penetration by LBE and dissolution of constituent metals into LBE.

Fig. 3c–h show the results of high chromium steels specimens. The specimens were tested at the same time and under the same conditions as the Al–Fe-coated SUS316FR specimen. However, opposite behavior with the Al–Fe-coated SUS316FR result, the corrosion attack mechanism of LBE into the high chromium steels matrix was observed as shown in Fig. 3c–h. The figures show that lead–bismuth penetrated into the matrix of SUS430, Recloy10, and NTK04L steels with up to 50, 150, and 55 μm in depth, respectively. There was no oxide layer formed on the surface of the SUS430, Recloy10, and NTK04L to protect from the penetration of LBE. Moreover, Fig. 3d, f, and h shows that the constituent metals of the matrixes dissolved into LBE. The results showed that high Cr steels SUS430, Recloy10, and NTK04L are not resistant to the corrosion attack of LBE at temperature of 700 °C.

3.2. Corrosion test in lead

Fig. 4a–l shows the SEM-EDX micrographs of the cross section of the tested specimens after immersion in molten lead for 500 h. Fig. 4a shows the SEM micrograph of the cross section of Al–Fe-coated STBA26. It is found that the coating layer of about 10 μm in thickness still remained on the surface of the STBA26 specimen with no penetration of lead. Moreover, peaks of oxygen, aluminum, and chromium are indicated on the surface of coating layer as shown in Fig. 4b. The peak of oxygen atoms on the surface suggested that a very thin oxide layer was formed on the surface of the coating layer. The oxygen concentration in lead of this experiment was 4.5×10^{-7} wt.% which was higher than the formation potentials of aluminum oxide and chromium oxide at 700 °C. Therefore, alumina oxide, and chromium oxide were possibly formed during immersion in lead. The oxide layer protected the surface of coating layer from penetration by lead and dissolution of constituent metals into lead. Fig. 4b exhibits that no presence of Al, Cr, Fe, and Ni peaks in the adhered lead were observed.

In order to make a comparison analysis, the STBA26 as received was tested at the same time and under the same conditions as the Al–Fe-coated STBA26 specimen. Opposite behavior to Al–Fe-coated STBA26, penetration of lead into the matrix of the specimen occurred as shown in Fig. 4c. The figure reveals that lead penetrated into the matrix with up to ~20 μm in depth. Moreover, no oxide layer as a barrier was formed to protect the surface from corrosion attack by lead. Dissolution of constituent metals from the matrix into lead occurred as shown in Fig. 4d. The results showed that high Cr STBA26 steel is not resistant to the corrosion attack of lead at the temperature of 700 °C.

The results of refractory metals tungsten and molybdenum are presented in Fig. 4e, f, g, and h, respectively. Fig. 4e reveals that

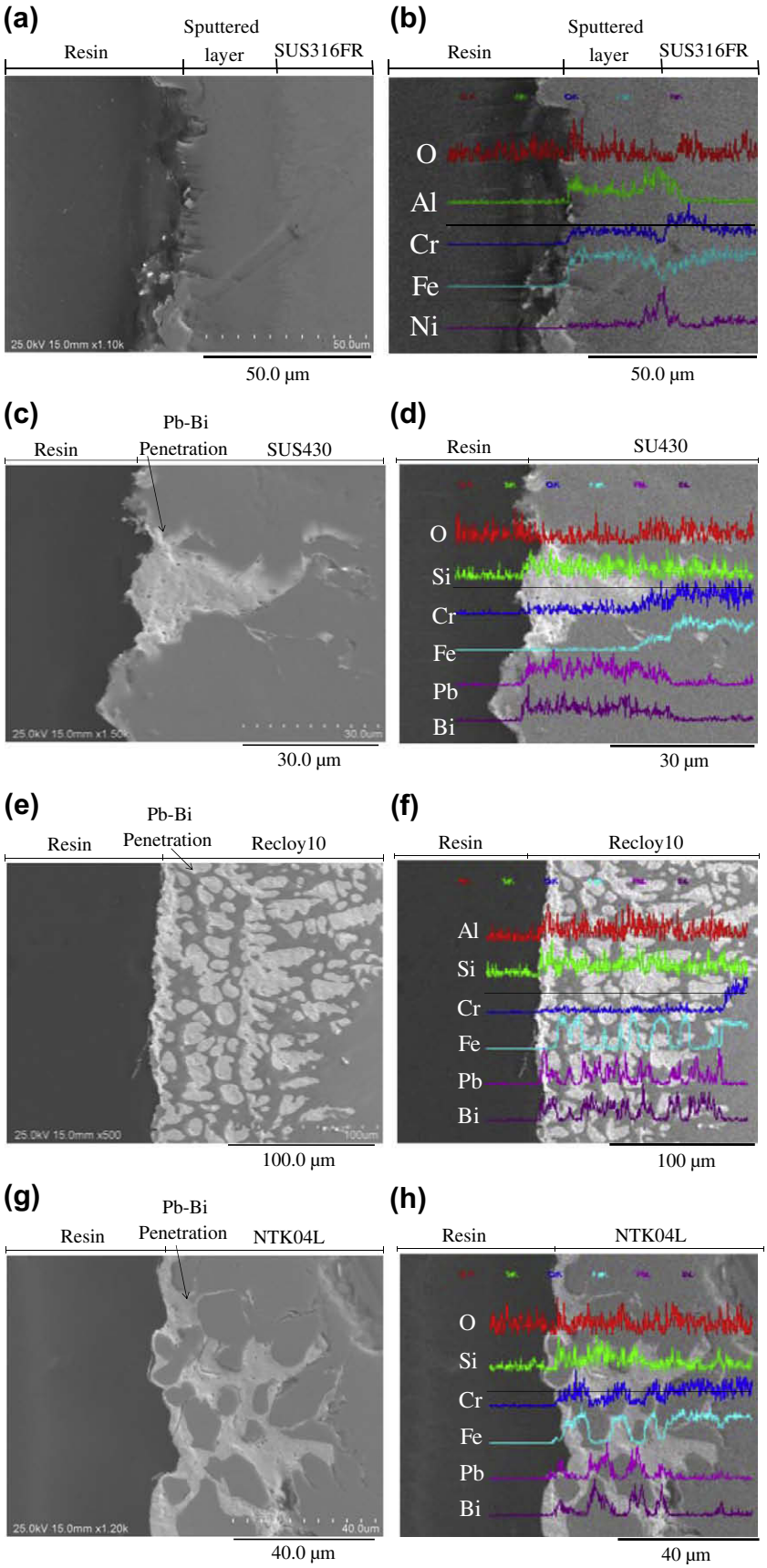

Fig. 3. SEM-EDX micrograph of cross section of tested specimens after immersion in lead–bismuth eutectic at 700 °C for 1000 h. (a) SEM micrograph of Al–Fe-coated SUS316FR. (b) EDX micrograph of Al–Fe-coated SUS316FR. (c) SEM micrograph of SUS430. (d) EDX micrograph of SUS430. (e) SEM micrograph of Recloy10. (f) EDX micrograph of Recloy10. (g) SEM micrograph of NTK04L. (h) EDX micrograph of NTK04L.

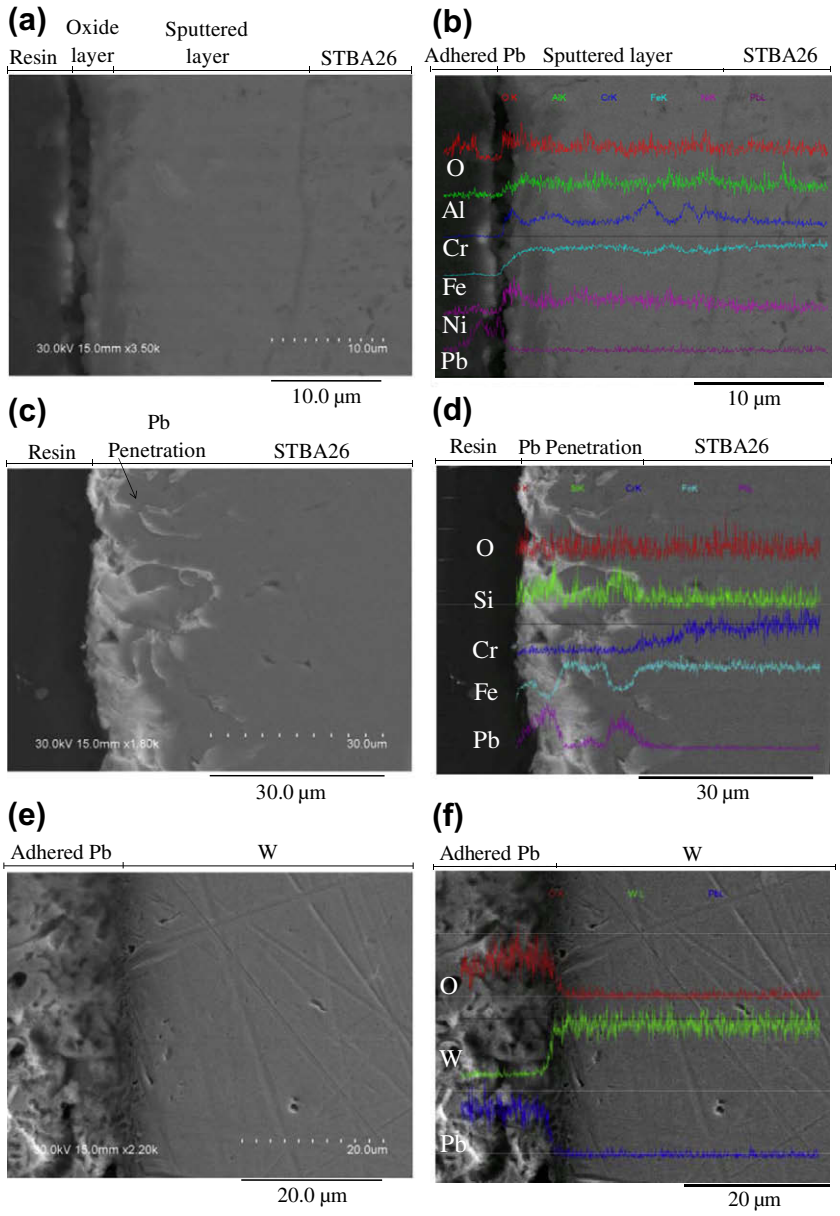

Fig. 4. SEM-EDX micrograph of cross section of tested specimens after immersion in lead at 700 °C for 500 h. (a) SEM micrograph of Al–Fe-coated STBA26. (b) EDX micrograph of Al–Fe-coated STBA26 (c) SEM micrograph of STBA26. (d) EDX micrograph of STBA26. (e) SEM micrograph of tungsten. (f) EDX micrograph of tungsten. (g) SEM micrograph of molybdenum. (h) EDX micrograph of molybdenum. (i) SEM micrograph of SiC. (j) EDX micrograph of SiC. (k) SEM micrograph of Ti_3SiC_2. (l) EDX micrograph of Ti_3SiC_2.

there was no penetration of lead into the tungsten matrix. Moreover, there were neither cracks nor a friable tungsten oxide layer on the surface of the specimen occurred. Furthermore, the result showed that neither dissolution of tungsten from the matrix into lead nor penetration of lead into the matrix of the specimen occurred as shown in Fig. 4f. As for the molybdenum specimen, Fig. 4g reveals that no penetration of lead into the molybdenum matrix was observed. Moreover, the figure shows that neither cracks nor a friable molybdenum oxide layer on the surface of the specimen occurred. Furthermore, Fig. 4h reveals that neither dissolution of molybdenum from the matrix into lead nor penetration of lead into the matrix of the specimen took place.

The results of ceramics SiC and Ti_3SiC_2 are presented in Fig. 4i–l, respectively. Fig. 4i reveals that there was no penetration of lead into the SiC matrix. Moreover, there were no cracks on the surface of the specimen occurred. Furthermore, Fig. 4j reveals that neither dissolution of silicon from the matrix into lead nor penetration of lead into the matrix of the specimen occurred. As for Ti_3SiC_2 specimen, Fig. 4k shows that there was no penetration of lead into the Ti_3SiC_2 matrix. Moreover, there were no cracks on the surface of the specimen occurred. Furthermore, Fig. 4l reveals that neither dissolution of titanium and silicon from the matrix of the specimen into lead nor penetration of lead into the matrix of the specimen took place.

4. Discussion

Good corrosion resistance of surface treatment using Al alloy to protect the steel surface from corrosion by LBE and lead with various treatments and techniques have been reported by several researchers [4–10]. Surface treatment steels to protect the steels surface from corrosion attack of LBE and lead can be done by several techniques. However, the corrosion resistance of Al alloying surface treat specimens in LBE and lead depends on the treatment technique. UBM sputtering technique has been widely used for all

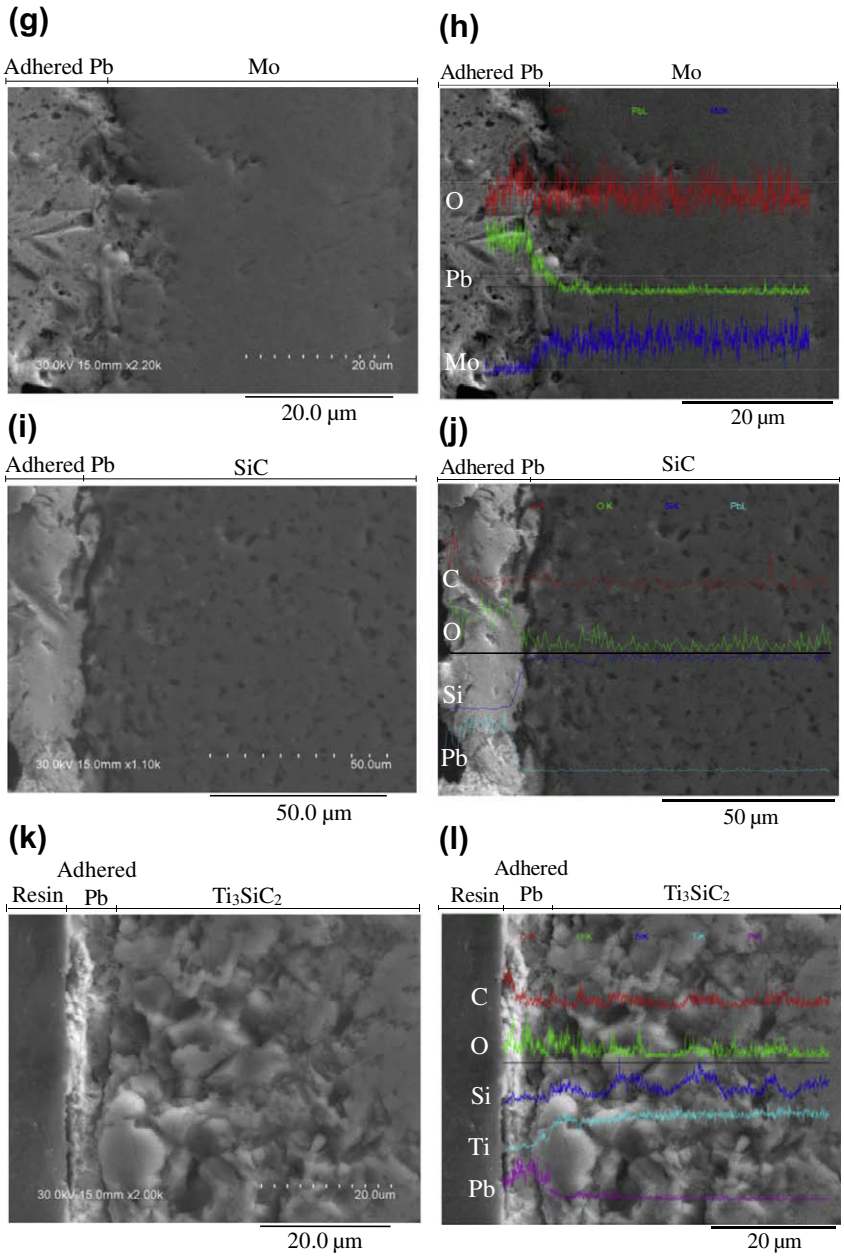

Fig. 4 (*continued*)

manner of mechanical, electrical and optical applications to deposit adherent, fully dense films for pure metals and alloys [23–26]. However, investigations of the effectiveness of the UBM sputtering technique to protect the steel from corrosion attack of LBE and lead have been few. The present investigations showed that coating layer still remain intact on the surface of SUS316FR and STBA26 without penetration of LBE and lead, respectively, after immersion at 700 °C. Moreover, a very thin oxide layer was formed on the surface of the coating layer. The thin oxide layer was stable at least for 1000 h in LBE at 700 °C and 500 h in lead at 700 °C, and effective to protect the surface from corrosion attack by LBE and lead. The formation and behavior of the thin oxide layer on the surface of an aluminized steel agrees with others report [6,7,10]. Further investigation for longer time is needed to clarify the stability of the oxide layer and the corrosion resistance of the coating layer.

Related to the results of high chromium steels, it was reported that SUS430, Recloy10, NTK04L, and STBA26 specimens exhibited good corrosion resistance with formation of multiple oxide layers in flowing lead–bismuth at 550 °C [11–14]. However, penetration of lead–bismuth into the SUS430, Recloy10, and NTK04L materials, and penetration of lead into the STBA26 material was found after the materials tested in LBE and lead at 700 °C. Moreover, there was no oxide layer on the surface of the steels to protect from corrosion attack of LBE and lead. These results show that high Cr SUS430, Recloy10, and NTK04L not withstand corrosion attack by LBE at 700 °C, and STBA26 not withstand corrosion attack by lead at 700 °C. Generally, ordinary feritic–martensitic steels are not compatible with LBE and lead at 700 °C. Therefore, advanced steels or surface-treated steels are needed for high temperature lead alloys nuclear systems. As for comparison with the ordinary high Cr ferritic-martensitic steels, it is evident that the Al–Fe coating with UBM sputtering able to protect the steels from corrosion attack by LBE and lead at 700 °C.

Tungsten and molybdenum are well known for their low solubility in liquid lead alloys environment. High corrosion resistance of tungsten and molybdenum in high temperature lead alloy which was revealed in this investigation agrees with the other report [10]. Nevertheless, it was reported that in high oxygen concentration tungsten oxide (WO_3) formed and reacted with liquid lead leading to the formation of friable Pb–W–O ternary compounds [18]. However, in the present investigation the results showed that there was no formation of tungsten oxide layer on the surface of the tungsten specimen because of relatively low oxygen concentration of lead in this corrosion test. Nevertheless, because of relatively short duration of corrosion test in the present study therefore further investigation for longer time is needed to clarify formation of tungsten oxide layer.

SiC and Ti_3SiC_2 showed high corrosion resistance in lead at 700 °C because of their low solubility in lead. Good corrosion result of the SiC in lead at 700 °C agrees with the report of SiC material tested in stagnant lead–bismuth at 700 °C [10]. However, in flowing lead–bismuth at 550 °C it was reported that cracks on the surface layer of SiC specimen with 25 mm in depth [11]. Recently, investigations of a new type of ceramic, Ti_3SiC_2, in high temperature lead alloys have been reported [10,20,21]. One of important advantages of these ternary carbides is that they readily machinable with nothing more sophisticated than a manual hack saw [22]. Compatibility of Ti_3SiC_2 in high temperature lead in this investigation agrees with the other reports [10,20,21].

5. Conclusions

The corrosion resistance of Al–Fe-coated steels using UBM sputtering technique, high chromium steels, refractory metals, and ceramics has been investigated in LBE and lead at 700 °C. From the investigation and analyses, it can be concluded that:

1. The Al–Fe coating layer using UBMS technique could remain on the surface of SUS316FR and STBA26 without penetration of LBE and lead, respectively. A very thin and stable oxide layer is formed on the surface of the coating layer, and protects the surface from corrosion attack of LBE and lead.
2. The high chromium steels SUS430, Recloy10, NTK04L, and STBA26 are not compatible for high temperature lead alloys at 700 °C.
3. Refractory metals molybdenum and tungsten, and ceramics SiC and Ti_3SiC_2 exhibit high corrosion resistance to high temperature liquid lead at 700 °C.

Acknowledgement

The authors would like to express their gratitude to Mr. T. El-Raghy, Ph.D. of 3-ONE-2 LLC for his supply of Ti_3SiC_2.

References

[1] B.F. Gromov, Y.I. Orlov, P.N. Martynov, V.A. Gulevsky, in: Proceedings of Heavy Liquid Metal Coolant (HLMC), 1999, p. 87.
[2] M. Takahashi, H. Sekimoto, K. Ishikawa, T. Suzuki, K. Hata, S. Que, S.Yoshida, T. Yano, M. Imai, in: Proceedings of the 10th International Conference on Nuclear Engineering (ICONE10), Arlington, Virginia, USA, ICONE10-22226, 14–18 April 2002.
[3] E.P. Loewen, A.T. Tokuhiro, J. Nucl. Sci. Technol. 40 (8) (2003) 614.
[4] G. Müller, A. Heinzel, J. Konys, G. Schumacher, A. Weisenburger, F. Zimmermann, V. Engelko, A. Rusanov, V. Markov, J. Nucl. Mater. 301 (2002) 40.
[5] G. Müller, A. Heinzel, J. Konys, G. Schumacher, A. Weisenburger, F. Zimmermann, V. Engelko, A. Rusanov, V. Markov, J. Nucl. Mater. 335 (2004) 163.
[6] G. Müller, G. Schumacher, F. Zimmermann, J. Nucl. Mater. 278 (2000) 85.
[7] A. Heinzel, M. Kondo, M. Takahashi, J. Nucl. Mater. 350 (2006) 264.
[8] Y. Kurata, M. Futakawa, S. Saito, J. Nucl. Mater. 335 (2004) 501.
[9] Ph. Deloffre, F. Balbaud-Célérier, A. Terlain, J. Nucl. Mater. 335 (2004) 180.
[10] A.K. Rivai, M. Takahashi, Progr. Nucl. Eng. 50 (2008) 560.
[11] M. Takahashi, M. Kondo, in: Proceeding of GLOBAL2005, Tsukuba, Japan, October 9–13, 2005, p. 425.
[12] M. Kondo, M. Takahashi, N. Sawada, K. Hata, J. Nucl. Sci. Technol. 43 (2) (2006) 107.
[13] M. Kondo, M. Takahashi, T. Suzuki, K. Ishikawa, K. Hata, S. Qiu, H. Sekimoto, J. Nucl. Mater. 343 (2005) 349.
[14] M. Kondo, M. Takahashi, J. Nucl. Mater. 356 (2006) 203.
[15] Y. Kurata, M. Futakawa, S. Saito, J. Nucl. Mater. 343 (2005) 333.
[16] T. Furukawa, G. Müller, G. Schumacher, A. Weisenburger, A. Heinzel, F. Zimmermann, K. Aoto, J. Nucl. Sci. Technol. 41 (3) (2004) 265.
[17] R.C. Asher, D. Davies, S.A. Beetham, Corros. Sci. 17 (1977) 545.
[18] G. Benamati, P. Buttol, V. Imbeni, C. Martini, G. Palombarini, J. Nucl. Mater. 279 (2000) 308.
[19] K. Hata, M. Takahashi, in: Proceeding of GLOBAL2005, Tsukuba, Japan, October 9–13, 2005, p. 446.
[20] L.A. Barnes, N.L. Dietz Rago, L. Leibowitz, J. Nucl. Mater. 373 (2008) 424.
[21] A. Heinzel, G. Müller, A. Weisenburger, J. Nucl. Mater. 392 (2009) 255.
[22] M.W. Barsoum, L.H. Ho-Duc, M. Radovic, T. El-Raghy, J. Electrochem. Soc. 150 (4) (2003) B166.
[23] R.I. Bates, R.D. Arnell, Surf. Coat. Technol. 89 (1997) 204.
[24] B. Window, N. Savvides, J. Vac. Sci. Technol. A 4 (2) (1986) 196.
[25] B. Window, N. Savvides, J. Vac. Sci. Technol. A 4 (3) (1986) 453.
[26] N. Savvides, B. Window, J. Vac. Sci. Technol. A 4 (3) (1986) 504.